Ivo Senjanović*, Marko Tomić, Smiljko Rudan and Neven Hadžić

Conforming shear-locking-free four-node rectangular finite element of moderately thick plate

DOI 10.1515/jmbm-2017-0001

Abstract: An outline of the modified Mindlin plate theory, which deals with bending deflection as a single variable, is presented. Shear deflection and cross-section rotation angles are functions of bending deflection. A new four-node rectangular finite element of moderately thick plate is formulated by utilizing the modified Mindlin theory. Shape functions of total (bending + shear) deflections are defined as a product of the Timshenko beam shape functions in the plate longitudinal and transversal direction. The bending and shear stiffness matrices, and translational and rotary mass matrices are specified. In this way conforming and shear-locking-free finite element is obtained. Numerical examples of plate vibration analysis, performed for various combinations of boundary conditions, show high level of accuracy and monotonic convergence of natural frequencies to analytical values. The new finite element is superior to some sophisticated finite elements incorporated in commercial software.

Keywords: conformity; finite element formulation; modified Mindlin plate theory; shear-locking.

1 Introduction

Plates are structural elements of many engineering structures, like bridges, ships, aircrafts, etc. Plates are classified into three categories depending on thickness-span ratio: thin plates, $h/L < 0.01$, moderately thick plates, $0.01 < h/L < 0.2$, and thick plates, $h/L > 0.2$. Structural analysis (strength, vibration, buckling) of thin plates has been performed within the well-known Kirchhoff plate theory [1], while moderately thick plates are analysed by the Mindlin plate theory as a 2D problem [2, 3]. Thick plates are considered to be an elastic body analysed by 3D theory of elasticity.

Dynamic behaviour of moderately thick plates is a more complex problem than that of thin plates, since influences of shear and rotary inertia are taken into account. The Mindlin theory deals with a system of three differential equations of motion in terms of three independent variables, i.e. deflection and two angles of cross-section rotation. A large number of papers has been published on this challenging problem and a comprehensive literature survey up to 1994 can be found in [4].

Generally speaking, there are two approaches to analysis of structural problems of moderately thick plates, i.e. analytical methods for solving differential equations of motion and numerical procedures based on the Rayleigh-Ritz energy method as well as the finite element method (FEM). Different analytical methods have been developed depending on which independent variables are selected as fundamental ones in the reduction of the system of differential equations of motion. Some methods operate with three, two or even one variable, as shown in [5–7], respectively. Developed analytical methods for vibration analysis of simply supported plates are relatively simple, as well as those for plates with simply supported two opposite edges. For vibration analysis of plates with any combination of simply supported and clamped edges a sophisticated closed-form solution is presented in [8].

The Rayleigh-Ritz method is widely used for vibration analysis of plates with arbitrary boundary conditions (simply supported, clamped and free) as well as with elastically supported edges. The achieved level of accuracy and convergence of solution depend on the chosen set of coordinate functions for definition of natural modes. Usually, two dimensional polynomials [9], or static deflection functions of the Timoshenko beam, [10], are used. An efficient solution is also achieved by applying the assumed mode method [11, 12].

The finite element method is a universal numerical tool for structural analysis of complex engineering structures concerning both the topology and material properties. A few triangular, rectangular and quadrilateral finite elements with different number of nodes have

***Corresponding author: Ivo Senjanović,** University of Zagreb, Faculty of Mechanical Engineering and Naval Architecture, Zagreb, Croatia, e-mail: ivo.senjanovic@fsb.hr

Marko Tomić, Smiljko Rudan and Neven Hadžić: University of Zagreb, Faculty of Mechanical Engineering and Naval Architecture, Zagreb, Croatia

been developed for Mindlin plate and incorporated in the library of commercial FEM software. Generally, the elements deal with three independent displacement fields, i.e. deflection and two cross-section rotations. They are prescribed by polynomials of the same order and in transition from thick to thin plate it is not possible to capture pure bending modes and zero shear strain constraints. In order to overcome this shear-locking problem in the FEM analysis, a few procedures have been developed, which are referred in [13]: reduced integration for shear terms [14, 15], which is commonly used in commercial software; mixed formulation of hybrid finite elements [16–18]; Assumed Natural Strain [19–21]; and Discrete Shear Gap (DSG) [22]. Recently, a new shear-locking-free finite element formulation for static analysis of moderately thick plates has been proposed, based on an extension of the Kirchhoff thin plate theory [13].

In order to overcome the above problems, the Mindlin theory has been modified [23]. The system of three governing differential equations of motion is reduced to a single equation with bending deflection as a potential function for determining shear deflection and cross-section rotation angles. By employing the modified Mindlin theory a new finite element formulation for moderately thick plates is presented in [24, 25]. Four-node rectangular finite element and three-node triangular finite element are worked out utilizing polynomial shape (interpolation) functions. The stiffness matrix, consisting of the bending stiffness matrix and the shear stiffness matrix, as well as the mass matrix, are developed. In this formulation the shear stiffness matrix of a thin plate becomes negligible compared to the bending stiffness matrix. Hence, the developed finite elements are shear-locking-free.

The above two finite elements are non-conforming since compatibility conditions of displacements are satisfied only in the nodes of the adjacent finite elements. As a result, convergence of natural frequencies is not monotonous. Therefore, in this paper a conforming four-node rectangular finite element is presented, which satisfies compatibility conditions along all edges of the adjacent finite elements. Shape functions of plate defection are defined as a product of the Timoshenko beam shape functions in longitudinal and transversal direction. The bending and shear stiffness matrices, as well as the transversal and rotary mass matrices are derived in a relatively simple way by employing an ordinary variational formulation [21]. The finite element is shear-locking-free and values of natural frequencies monotonously converge to exact solution from above.

2 Outline of the modified Mindlin theory

Displacements of a thick plate, i.e. total deflection, w, and angles of rotations, ψ_x, ψ_y, are shown in Figure 1 in the Cartesian coordinate system. The basic idea of the modified Mindlin thick plate theory is, like in case of the modified Timoshenko beam theory [26], decomposition of the total deflection into bending deflection and shear deflection

$$w(x, y, t) = w_b(x, y, t) + w_s(x, y, t). \tag{1}$$

Rotations of the plate cross-sections are caused only by bending, and one can write for rotation angles

$$\psi_x = -\frac{\partial w_b}{\partial x},\ \psi_y = -\frac{\partial w_b}{\partial y}. \tag{2}$$

Bending moments and twist moments are results of plate curvature and warping, respectively

$$\begin{aligned} M_x &= -D\left(\frac{\partial^2 w_b}{\partial x^2} + \nu\frac{\partial^2 w_b}{\partial y^2}\right),\\ M_y &= -D\left(\frac{\partial^2 w_b}{\partial y^2} + \nu\frac{\partial^2 w_b}{\partial x^2}\right),\\ M_{xy} &= M_{yx} = -(1-\nu)D\frac{\partial^2 w_b}{\partial x \partial y}, \end{aligned} \tag{3}$$

where

$$D = \frac{Eh^3}{12(1-\nu^2)}, \tag{4}$$

is the plate flexural rigidity, and h, E and ν is plate thickness, Young's modulus of elasticity and Poisson's ratio, respectively.

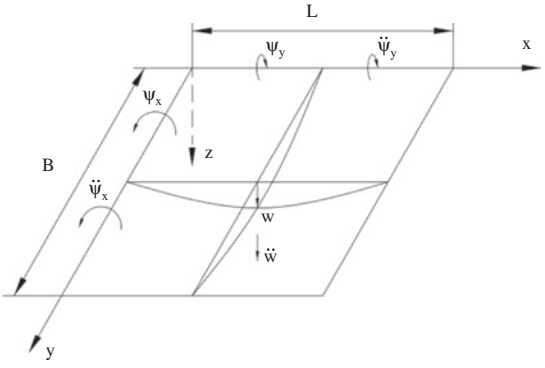

Figure 1: Displacements of rectangular plate.

Shear strain is defined as summation of the plate generatrix rotation and cross-section rotation, i.e.

$$\gamma_x = \frac{\partial w}{\partial x} + \psi_x = \frac{\partial w_s}{\partial x},$$
$$\gamma_y = \frac{\partial w}{\partial y} + \psi_y = \frac{\partial w_s}{\partial y}. \tag{5}$$

As a result the shear forces read

$$Q_x = S\frac{\partial w_s}{\partial x},\ Q_y = S\frac{\partial w_s}{\partial y}, \tag{6}$$

where $S = k_s G h$ is shear rigidity and k_s is shear correction coefficient.

Plate natural vibrations are performed under action of distributed inertia force and bending moments

$$q = \bar{m}\frac{\partial^2 w}{\partial t^2},\quad m_x = -J\frac{\partial^3 w_b}{\partial x \partial t^2},\ m_y = -J\frac{\partial^3 w_b}{\partial y \partial t^2}, \tag{7}$$

where $\bar{m} = \rho h$ is the plate mass per unit area, $J = \rho I = \rho h^3/12$ is the mass moment of inertia of the cross-section per unit breadth, h is the plate thickness and ρ is mass density.

Consideration of the equilibrium of vertical forces and moments around the x and y axis, by applying the above relations, leads to a single differential equation of motion in terms of bending deflection

$$D\Delta\Delta w_b - J\left(1 + \frac{D\bar{m}}{SJ}\right)\frac{\partial^2}{\partial t^2}\Delta w_b + \bar{m}\frac{\partial^2}{\partial t^2}\left(w_b + \frac{J}{\bar{m}S}\frac{\partial^2 w_b}{\partial t^2}\right) = q_e(x, y, t), \tag{8}$$

where $\Delta(.) = \frac{\partial^2(.)}{\partial x^2} + \frac{\partial^2(.)}{\partial y^2}$ is the Laplace differential operator and q_e is distributed excitation load. Once bending deflection w_b is determined the total deflection (1) is obtained by the following formula [23]

$$w = w_b + \frac{J}{S}\frac{\partial^2 w_b}{\partial t^2} - \frac{D}{S}\Delta w_b. \tag{9}$$

Final plate deformation depends on boundary conditions.

3 Formulation of shape functions

The four-node rectangular finite element with three degrees of freedom (d.o.f.) per node is considered, Figure 2. The dimensionless coordinates $\xi = x/a$ and $\eta = y/b$ are introduced due to reason of simplicity. The shape (interpolation) functions of plate deflection are assumed in the form of products of thick beam shape functions, based on the modified Timoshenko beam theory [26], $X_i(\xi)$ and $Y_j(\eta)$, i, j = 1, 2, 3, 4, in x and y direction respectively

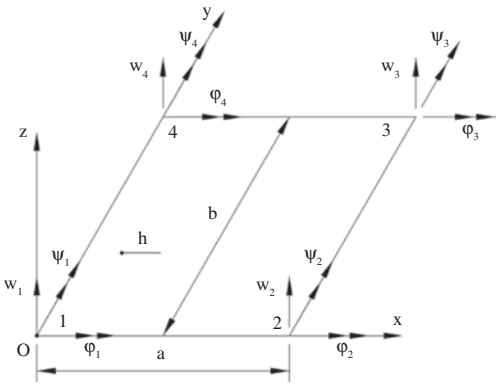

Figure 2: Rectangular finite element with nodal displacements.

Node 1	Node 2	Node 3	Node 4
$\Phi_1 = X_1Y_1$	$\Phi_4 = X_3Y_1$	$\Phi_7 = X_3Y_3$	$\Phi_{10} = X_1Y_3$
$\Phi_2 = X_1Y_2$	$\Phi_5 = X_3Y_2$	$\Phi_8 = X_3Y_4$	$\Phi_{11} = X_1Y_4$
$\Phi_3 = -X_2Y_1$	$\Phi_6 = -X_4Y_1$	$\Phi_9 = -X_4Y_3$	$\Phi_{12} = -X_2Y_3$.

(10)

The beam shape functions, which take both shear stiffness and rotary inertia into account, are specified in Appendix A.

Each of 12 shape functions $\Phi_k(\xi, \eta) = X_i(\xi)Y_j(\eta)$, where indexes i and j appear in combinations (10), can be expanded into beam bending and shear terms, and mixed bending and shear terms

$$\Phi_k = X_iY_j = (X_{ib} + X_{is})(Y_{jb} + Y_{js}) = X_{ib}Y_{jb} + X_{ib}Y_{js} + X_{is}Y_{jb} + X_{is}Y_{js}. \tag{11}$$

The beam bending and shear shape functions are also given in Appendix A. Hence, each of plate shape functions consists of four displacement fields, i.e. bending in both x and y direction, $X_{ib}Y_{jb}$; bending in x and shear in y direction, $X_{ib}Y_{js}$, and vice versa, $X_{is}Y_{jb}$; and shear in both directions, $X_{is}Y_{js}$.

In order to formulate finite element bending and shear stiffness matrix it is necessary to decompose bending and shear shape functions (11), as in the case of non-conforming finite element [24, 25]. Unfortunately, this is not possible in the considered case. However, cross-section rotation angles and shear angles, which are caused by bending and shear respectively, can be extracted from (11)

$$\Psi_{xk} = -\frac{1}{a} X'_{ib} Y_j,\ \Psi_{yk} = -\frac{1}{b} X_i Y'_{jb}, \tag{12}$$

$$\Gamma_{xk} = \frac{1}{a} X'_{is} Y_j,\ \Gamma_{yk} = \frac{1}{b} X_i Y'_{js}. \tag{13}$$

Hence, for derivation of all finite element properties it is necessary to operate with the known shape functions of total deflection (11) and rotation and shear angles (12) and (13), respectively.

The first two deflection shape functions of the present conforming and non-conforming finite element of aspect ratio $a/b=1$ and thickness-span ratio $h/b=1.6$, Appendix B, are shown in Figure 3. High value of h/b is a result of plate thickness-span ratio $h/B=0.2$ and the finite element mesh 8×8. The first shape function of non-conforming finite element is very close to that of conforming element, while the difference between the second shape functions are relatively large.

4 Bending and shear stiffness matrix

For derivation of bending and shear stiffness matrix the ordinary finite element technique is used. Finite element

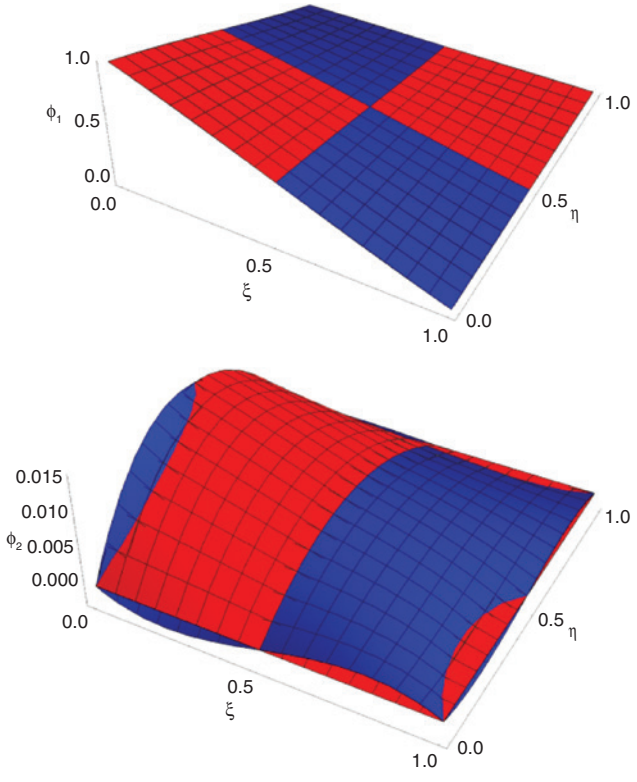

Figure 3: The first two deflection shape functions, $a/b=1$, $h/b=1.6$: red – conforming element, blue – non-conforming element.

deflection is expressed as product of deflection shape functions and nodal displacements

$$w(\xi,\eta) = \langle \Phi_k(\xi,\eta)\rangle\{\delta\},\quad k=1,\ 2\ldots12, \tag{14}$$

where according to Figure 2

$$\{\delta\} = \{\{\delta\}_l\},\quad \{\delta\}_l = \begin{Bmatrix} w_l \\ \phi_l \\ \psi_l \end{Bmatrix},\quad l=1,\ 2,\ 3,\ 4. \tag{15}$$

In a similar way one can write for rotation angles

$$\begin{aligned} \psi_x(\xi,\eta) &= \langle \Psi_{xk}(\xi,\eta)\rangle\{\delta\}, \\ \psi_y(\xi,\eta) &= \langle \Psi_{yk}(\xi,\eta)\rangle\{\delta\}, \end{aligned} \tag{16}$$

and shear angles

$$\begin{aligned} \gamma_x(\xi,\eta) &= \langle \Gamma_{xk}(\xi,\eta)\rangle\{\delta\}, \\ \gamma_y(\xi,\eta) &= \langle \Gamma_{yk}(\xi,\eta)\rangle\{\delta\}. \end{aligned} \tag{17}$$

According to (3) the finite element bending curvature and warping can be presented as vector

$$\{\kappa\} = \begin{Bmatrix} \dfrac{\partial \psi_x}{\partial x} \\ \dfrac{\partial \psi_y}{\partial y} \\ \dfrac{\partial \psi_x}{\partial y} + \dfrac{\partial \psi_y}{\partial x} \end{Bmatrix} \tag{18}$$

By substituting (12) into (16), and taking (18) into account, yields

$$\{\kappa\} = -[L]_b\{\delta\}, \tag{19}$$

where

$$[L]_b = \begin{bmatrix} \dfrac{1}{a^2}\langle (X''_{ib} Y_j)_k \rangle \\ \dfrac{1}{b^2}\langle (X_i Y''_{jb})_k \rangle \\ \dfrac{1}{ab}\langle (X'_{ib} Y'_j)_k + (X'_i Y'_{jb})_k \rangle \end{bmatrix}. \tag{20}$$

By using a general formulation of stiffness matrix from the finite element method based on variational principle [21], one can write for bending stiffness matrix

$$[K]_b = ab\int_0^1\int_0^1 [L]_b^T [D]_b [L]_b \mathrm{d}\xi \mathrm{d}\eta, \tag{21}$$

where

$$[D]_b = D\begin{bmatrix} 1 & \nu & 0 \\ \nu & 1 & 0 \\ 0 & 0 & \dfrac{1-\nu}{2} \end{bmatrix} \tag{22}$$

Elements of matrix $[K]_b$, after multiplication of the subintegral matrices, can be presented in the form

$$K_{kl}^b = \frac{D}{ab}\int_0^1\int_0^1 \left\{ p_k\left[\left(\frac{b}{a}\right)^2 p_l + \nu q_l\right] + q_k\left[\left(\frac{a}{b}\right)^2 q_l + \nu p_l\right] + \frac{1-\nu}{2} r_k r_l \right\} \mathrm{d}\xi\,\mathrm{d}\eta, \tag{23}$$

where, according to (20)

$$p_k = (X_{ib}'' Y_j)_k,\ q_k = (X_i Y_{jb}'')_k, \quad r_k = (X_{ib}' Y_j')_k + (X_i' Y_{jb}')_k. \tag{24}$$

Related to the shear stiffness the shear strain vector according to (5) reads

$$\{\gamma\} = \begin{Bmatrix} \gamma_x \\ \gamma_y \end{Bmatrix}. \tag{25}$$

By substituting (13) into (17), and then into (25), yields

$$\{\gamma\} = [L]_s\{\delta\}, \tag{26}$$

where

$$[L]_s = \begin{bmatrix} \dfrac{1}{a}\langle (X_{is}' Y_j)_k \rangle \\ \dfrac{1}{b}\langle (X_i Y_{js}')_k \rangle \end{bmatrix} \tag{27}$$

Analogously to (21) one can write for the shear stiffness matrix

$$[K]_s = ab\int_0^1\int_0^1 [L]_s^T [D]_s [L]_s \mathrm{d}\xi\,\mathrm{d}\eta, \tag{28}$$

where

$$[D]_s = S\begin{bmatrix} 1 & 0 \\ 0 & 1 \end{bmatrix} \tag{29}$$

is matrix of the plate shear rigidity. Since $[D]_s$ includes unit matrix, Eq. (28) is reduced to the form

$$[K]_s = Sab\int_0^1\int_0^1 [L]_s^T [L]_s \mathrm{d}\xi\,\mathrm{d}\eta \tag{30}$$

5 Translational and rotary mass matrix

According to the general formulation [21], mass matrix depends on deflection shape function Φ_k, Eq. (11), and one can write for the translational mass matrix

$$[M]_t = \bar{m}ab\int_0^1\int_0^1 \{(X_i Y_j)_k\}\langle (X_i Y_j)_k \rangle \mathrm{d}\xi\,\mathrm{d}\eta. \tag{31}$$

The beam shape functions X_i and Y_j are specified in Appendix A.

Mass matrix due to mass rotation is derived in the following way. According to (2) vector of cross-section rotation reads

$$\{\psi\} = \begin{Bmatrix} \psi_x \\ \psi_y \end{Bmatrix} \tag{32}$$

and taking into account (12) and (16), yields

$$\{\psi\} = -[L]_r\{\delta\}, \tag{33}$$

where

$$[L]_r = \begin{bmatrix} \dfrac{1}{a}\langle (X_{ib}' Y_j)_k \rangle \\ \dfrac{1}{b}\langle (X_i Y_{jb}')_k \rangle \end{bmatrix} \tag{34}$$

Rotary mass matrix is specified similarly to the shear stiffness matrix, Eq. (26)

$$[M]_r = ab\int_0^1\int_0^1 [L]_r^T [J][L]_r \mathrm{d}\xi\,\mathrm{d}\eta, \tag{35}$$

where

$$[\mathrm{J}] = J\begin{bmatrix} 1 & 0 \\ 0 & 1 \end{bmatrix}. \tag{36}$$

Hence, one can write

$$[M]_r = Jab\int_0^1\int_0^1 [L]_r^T [L]_r \mathrm{d}\xi\,\mathrm{d}\eta. \tag{37}$$

Finally, the finite element equation for natural vibration analysis of thick plate reads

$$(([K]_b + [K]_s) - \omega^2([M]_t + [M]_r))\{\delta\} = \{0\}, \tag{38}$$

where ω is natural frequency. Elements of shear stiffness matrix $[K]_s$, according to (27) and (A3), includes

Table 1: Frequency parameter $\mu = \omega a^2 \sqrt{\rho h / D}$ of square plate, case SSSS, $k_s = 0.86667$.

h/a	Method	1/11/	2/12/	3/21/	4/22/	5/13/	6/31/	7/23/	8/32/
0.001	Analytical[a]	19.739	49.348	49.348	78.956	98.694	98.694	128.302	128.302
	FEM-PC	20.257	50.294	50.294	81.558	100.057	100.057	132.576	132.576
	FEM-NC	19.579	48.738	48.738	76.599	97.484	97.484	123.372	123.372
	LS-DYNA	20.532	49.593	49.633	76.211	102.193	102.237	123.956	123.976
	NASTRAN	19.377	48.115	48.115	74.420	96.381	96.381	119.255	119.255
0.1	Analytical[a]	19.084	45.585	45.585	70.022	85.365	85.365	107.178	107.178
	FEM-PC	19.170	45.923	45.923	71.043	86.661	86.661	109.695	109.695
	FEM-NC	19.082	45.924	48.924	70.134	87.655	87.655	108.510	108.510
	LS-DYNA	18.555	45.342	45.342	67.045	87.710	87.764	102.712	102.712
	NASTRAN	18.274	44.047	44.047	64.502	83.076	83.132	97.071	97.071
0.2	Analytical[a]	17.506	38.385	38.385	55.586	65.719	65.719	79.476	79.476
	FEM-PC	17.576	38.775	38.775	56.529	67.465	67.465	81.956	81.956
	FEM-NC	17.408	38.331	38.331	55.216	66.851	66.851	79.959	79.959
	LS-DYNA	16.791	38.189	38.189	53.103	60.356	60.356	65.994	66.128
	NASTRAN	16.604	37.414	37.414	51.803	63.932	64.062	72.406	72.406

[a]Appendix C.

Table 2: Frequency parameter $\lambda = (\omega b^2 / \pi^2) \sqrt{\rho h / D}$ of rectangular plate, case CSCS, $a/b = 0.5$, $k_s = 0.86667$.

h/*b*	Method	1	2	3	4	5	6	7	8
0.01	Analytical[a]	9.622	11.691	15.777	22.076	25.573	27.891	30.545	31.969
	FEM-PC	9.701	12.000	16.438	23.207	25.704	28.389	32.317	33.171
	FEM-NC	9.505	11.283	15.052	21.128	25.272	26.715	29.558	29.615
	LS-DYNA	9.774	11.441	15.269	22.361	27.143	28.137	30.305	34.639
	NASTRAN	9.455	11.053	14.538	20.373	25.168	26.323	28.582	28.689
0.1	Analytical[a]	7.587	9.034	11.948	16.139	16.854	18.117	20.389	21.199
	FEM-PC	7.650	9.197	12.252	16.742	17.120	18.574	21.115	22.480
	FEM-NC	7.539	8.846	11.713	16.133	16.914	17.855	19.826	21.895
	LS-DYNA	7.726	9.008	11.852	16.172	17.364	18.002	19.326	21.271
	NASTRAN	7.541	8.723	11.269	14.920	16.765	17.313	18.418	18.929
0.2	Analytical[a]	5.202	6.223	8.261	10.350	10.898	11.209	12.706	13.809
	FEM-PC	5.309	6.431	8.572	10.592	11.514	11.597	13.262	15.094
	FEM-NC	5.235	6.252	8.363	10.526	11.329	11.360	12.853	14.954
	LS-DYNA	5.319	6.322	8.196	10.436	10.547	11.049	11.886	12.537
	NASTRAN	5.250	6.202	7.970	10.056	10.402	10.851	11.614	11.994

[a][8, 25].

parameters α and β, Eqs. (A4) and (A5), respectively. Their values are rapidly reduced for thin plate due to small thickness-span ratio h/a and h/b. In case of very thin plate shear stiffness matrix $[K]_s$ becomes negligible compared to bending stiffness matrix $\left[K\right]_b$ in (38). This fact indicates that the presented finite element is shear-locking-free. Assembling of the finite element Eqs. (38) is performed in ordinary way of the finite element technique [20, 21].

6 Illustrative numerical examples

The developed conforming four-node finite element is validated by three numerical examples of natural vibrations with different boundary conditions: simply supported square plate (SSSS), rectangular plate clumped on transverse edges and simply supported on longitudinal edges (CSCS), and rectangular plate with combined clamped, free, and simply supported boundaries (CFSS). All plates are modelled with $8\times 8=64$ finite elements. Value of plate aspect ratio, a/b, and shear correction factor, k_s, as well as formula for dimensionless frequency parameter μ or λ, are given in the title of Tables 1–3. Thin, moderately thick and thick plate, are considered. Values of frequency parameter determined by the present conforming finite element (FEM-PC), and those by non-conforming finite element (FEM-NC) [24, 25], are compared with analytical solution for case SSSS and CSCS, Tables 1 and 2. For boundary conditions CFSS, Table 3, solution obtained by the Rayleigh-Ritz method [9] is used as the referent one. FEM results agree very well with analytical ones. Between FEM-PC and FEM-NS results small difference can be noticed for thick plate.

The same boundary value problems are solved by commercial software LS-DYNA [27] and NASTRAN [28], for comparison. In the former case fully integrated shell

Table 3: Frequency parameter $\lambda=(\omega b^2/\pi^2)\sqrt{\rho h/D}$ of rectangular plate, case CFSS, $a/b=0.4$, $k_s=5/6$.

h/b	Method	1	2	3	4	5	6	7	8
0.001	RR[a]	9.874	11.346	14.900	19.539	26.624	31.698	33.397	35.788
	FEM-PC	9.924	11.691	15.380	21.184	29.225	31.793	33.830	38.057
	FEM-NC	9.896	11.175	14.028	18.772	25.615	31.712	32.677	34.680
	LS-DYNA	9.970	11.109	13.592	17.886	24.956	32.849	33.729	34.975
	NASTRAN	9.823	10.945	13.363	17.404	23.574	31.402	32.257	32.623
0.1	RR[a]	7.941	8.970	11.135	14.462	18.761	20.459	21.357	23.112
	FEM-PC	7.974	9.054	11.318	14.818	19.481	20.759	21.742	23.696
	FEM-NC	7.981	8.849	10.812	14.081	18.657	20.746	21.281	22.542
	LS-DYNA	8.123	8.952	10.755	13.690	17.651	21.058	21.439	22.021
	NASTRAN	7.985	8.635	10.196	12.825	16.215	19.771	20.457	20.887
0.2	RR[a]	5.594	6.305	7.752	9.828	12.294	12.679	13.236	14.289
	FEM-PC	5.625	6.365	7.877	10.109	12.917	12.949	13.539	14.711
	FEM-NC	5.624	6.219	7.592	9.809	12.715	12.948	13.364	14.255
	LS-DYNA	5.744	6.358	7.611	9.368	11.288	12.932	13.031	13.124
	NASTRAN	5.669	6.126	7.277	8.993	10.839	12.470	12.790	12.945

[a]Rayleigh-Ritz [9].

Table 4: Convergence pattern of frequency parameter $\mu=\omega a^2\sqrt{\rho h/D}$ of square plate, case SSSS, $a/b=1$, $h/a=0.2$, $k_s=0.86667$, FEM-PC.

FEM mesh	1/11/	2/12/	3/21/	4/22/	5/13/	6/31/	7/23/	8/32/
2×2	18.421	50.798	50.798	101.260	101.279	168.984	168.984	
4×4	17.761	39.899	39.899	59.206	72.369	72.369	88.744	88.744
6×6	17.627	39.072	39.072	57.246	68.812	68.812	83.857	83.857
8×8	17.576	38.775	38.775	56.529	67.465	67.465	81.956	81.956
10×10	17.551	38.636	38.636	56.192	66.836	66.836	81.064	81.064
Analytical[a]	17.506	38.385	38.385	55.586	65.719	65.719	79.476	79.476

[a]Appendix C.

Table 5: Convergence pattern of frequency parameter $\lambda=(\omega b^2/\pi^2)\sqrt{\rho h/D}$ of rectangular plate, case CSCS, $a/b=0.5$, $h/b=0.2$, $k_s=0.86667$, FEM-PC.

FEM mesh	1	2	3	4	5	6	7	8
2×2	5.680	7.242	11.315	16.976	18.050			
4×4	5.388	6.577	9.027	11.129	12.263	14.193	15.364	17.927
6×6	5.329	6.470	8.698	10.734	11.776	11.883	13.532	15.734
8×8	5.309	6.431	8.572	10.592	11.514	11.597	13.262	15.094
10×10	5.299	6.413	8.512	10.526	11.332	11.514	13.133	14.675
Analytical[a]	5.202	6.223	8.261	10.350	10.898	11.209	12.706	13.809

[a][8, 25].

Table 6: Convergence pattern of frequency parameter $\lambda=(\omega b^2/\pi^2)\sqrt{\rho h/D}$ of rectangular plate, case CFSS, $a/b=0.4$, $h/b=0.2$ $k_s=5/6$, FEM-PC.

FEM mesh	1	2	3	4	5	6	7	8
2×2	5.960	6.897	8.869	12.259	18.427	19.526	20.288	22.735
4×4	5.700	6.503	8.154	10.575	13.636	14.347	15.720	16.255
6×6	5.645	6.405	7.959	10.292	13.126	13.288	13.762	15.017
8×8	5.625	6.365	7.877	10.109	12.917	12.949	13.539	14.711
10×10	5.615	6.345	7.835	10.014	12.715	12.850	13.434	14.565
RR[a]	5.594	6.305	7.752	9.828	12.294	12.679	13.236	14.289

[a]Rayleigh-Ritz [9].

element with four nodes, based on the Reissner-Mindlin theory (ELFORM 16) is used, while in the latter case 2D four-node thick plate finite element is applied. The NASTRAN results are considerably lower than the analytical values for all three plate thickness, while those determined by LS-DYNA are somewhat higher for thin plate and lower for thick plate.

The convergence test is carried out for the thick plate and all three cases of boundary conditions, Tables 4–6. The finite element mesh density is increased from 2×2 to 10×10. It can be observed that values of frequency parameters in all three examples converge monotonically from above as the mesh density is increased. Convergence is faster for lower frequencies, since simple shape of corresponding natural modes can be successfully described by smaller number of finite elements.

7 Conclusion

An advantage of the modified Mindlin theory, outlined in Section 2, is dealing with only one variable, i.e. bending deflection as a potential function for determining total (bending + shear) deflection, cross-section rotation angles, strains and sectional forces. This enables a new finite element formulation for moderately thick plate by following the ordinary FEM procedure and ensuring in such a way variational consistency. The four-node rectangular finite element is defined by specifying the shape functions of the total deflection as a product of the Timosheko beam shape functions in longitudinal and transversal direction. In this way conformity of the finite elements is ensured, while the application of the Modified Mindlin theory results with shear-locking-free finite element.

As a result of the above two finite element characteristics, the illustrative numerical examples of thin and moderately thick plate with various boundary conditions show high level of accuracy and fast monotonous convergence of natural frequencies to the exact values from above. Moreover, this relatively simple finite element, in the most analysed cases, achieves a higher level of accuracy than the sophisticated finite elements incorporated in the used commercial software.

Acknowledgments: This investigation was done within the international collaborative project Global Core Research Center for Ships and Offshore Plants (GCRC SOP), established by the South Korean Government (MSIP) through the National Research Foundation of the South Korea (NRF). Therefore, the authors are grateful to both MSIP and NRF for the support under Grant No. 2011-0030013 signed in between NRF and University of Zagreb.

Appendix A

Beam shape functions

Total functions, $X_i = X_{ib} + X_{is}$

$$X_1 = \frac{1}{\lambda}[1-\xi^2(3-2\xi)+12\alpha(1-\xi)]$$
$$X_2 = \frac{a}{\lambda}\xi(1-\xi)(1-\xi+6\alpha)$$
$$X_3 = \frac{1}{\lambda}\xi[\xi(3-2\xi)+12\alpha]$$
$$X_4 = -\frac{a}{\lambda}\xi(1-\xi)(\xi+6\alpha). \tag{A1}$$

Bending functions, X_{ib}

$$X_{1b} = \frac{1}{\lambda}[1-\xi^2(3-2\xi)+6\alpha]$$
$$X_{2b} = \frac{a}{\lambda}[\xi(1-\xi)^2-2\alpha(2+6\alpha)+6\alpha\xi(2-\xi)]$$
$$X_{3b} = \frac{1}{\lambda}[\xi^2(3-2\xi)+6\alpha]$$
$$X_{4b} = -\frac{a}{\lambda}[\xi^2(1-\xi)+2\alpha(1-6\alpha)-6\alpha\xi^2)]. \tag{A2}$$

Shear functions, X_{is}

$$X_{1s} = \frac{2\alpha}{\lambda}3(1-2\xi)$$
$$X_{2s} = \frac{2a\alpha}{\lambda}(2-3\xi+6\alpha)$$
$$X_{3s} = -\frac{2\alpha}{\lambda}3(1-2\xi)$$
$$X_{4s} = \frac{2a\alpha}{\lambda}(1-3\xi+6\alpha), \tag{A3}$$

where

$$\alpha = \frac{D}{Sa^2} = \frac{1}{6(1-\nu)k_s}\left(\frac{h}{a}\right)^2,$$
$$\lambda = 1+12\alpha. \tag{A4}$$

Beam shape functions in y-direction, $Y_j = Y_{jb} + Y_{js}$, have the same form as those in x-direction, $X_i = X_{ib} + X_{is}$. It is only necessary to change argument ξ into η and use parameters β and μ instead of α and λ, where

$$\beta = \frac{D}{Sb^2} = \frac{1}{6(1-\nu)k_s}\left(\frac{h}{b}\right)^2,$$
$$\mu = 1+12\beta. \tag{A5}$$

Appendix B

Shape functions of the non-conforming finite element

The four-node thick plate finite element with compatible nodal displacements, based on the modified Mindlin theory, is presented in [24, 25]. Here, only shape functions are specified due to comparation to the conforming finite element.

Bending shape functions, shear shape functions and total deflection functions are given in matrix notation

$$\langle\Phi(\xi,\eta)_b\rangle = \langle P(\xi,\eta)\rangle_b[C]^{-1},$$
$$\langle\Phi(\xi,\eta)\rangle_s = \langle P(\xi,\eta)\rangle_s[C]^{-1},$$
$$\langle\Phi(\xi,\eta)\rangle = \langle\Phi(\xi,\eta)\rangle_b + \langle\Phi(\xi,\eta)\rangle_s, \tag{B1}$$

where

$$\langle P(\xi,\eta)\rangle_b = \langle 1 \;\; \xi \;\; \eta \;\; \xi^2 \;\; \xi\eta \;\; \eta^2 \;\; \xi^3 \;\; \xi^2\eta \;\; \xi\eta^2 \;\; \eta^3 \;\; \xi^3\eta \;\; \xi\eta^3 \rangle,$$
$$\langle P(\xi,\eta)\rangle_s = \langle 0 \;\; 0 \;\; 0 \;\; 2\alpha \;\; 0 \;\; 2\beta \;\; 6\alpha\xi \;\; 2\alpha\eta \;\; 2\beta\xi \;\; 6\beta\eta$$
$$6\alpha\xi\eta \;\; 6\beta\xi\eta \rangle. \tag{B2}$$

Parameters α and β are defined by formulae (A4) and (A5), respectively.

Matrix $[C]$ is of the following form

$$[C]=\begin{bmatrix}
1 & 0 & 0 & -2\alpha & 0 & -2\beta & 0 & 0 & 0 & 0 & 0 & 0\\
0 & 0 & \frac{1}{b} & 0 & 0 & 0 & 0 & 0 & 0 & 0 & 0 & 0\\
0 & -\frac{1}{a} & 0 & 0 & 0 & 0 & 0 & 0 & 0 & 0 & 0 & 0\\
1 & 1 & 0 & 1-2\alpha & 0 & -2\beta & 1-6\alpha & 0 & -2\beta & 0 & 0 & 0\\
0 & 0 & \frac{1}{b} & 0 & \frac{1}{b} & 0 & 0 & \frac{1}{b} & 0 & 0 & \frac{1}{b} & 0\\
0 & -\frac{1}{a} & 0 & -\frac{2}{a} & 0 & 0 & -\frac{3}{a} & 0 & 0 & 0 & 0 & 0\\
1 & 1 & 1 & 1-2\alpha & 1 & 1-2\beta & 1-6\alpha & 1-2\alpha & 1-2\beta & 1-6\beta & 1-6\alpha & 1-6\beta\\
0 & 0 & \frac{1}{b} & 0 & \frac{1}{b} & \frac{2}{b} & 0 & \frac{1}{b} & \frac{2}{b} & \frac{3}{b} & \frac{1}{b} & \frac{3}{b}\\
0 & -\frac{1}{a} & 0 & -\frac{2}{a} & -\frac{1}{a} & 0 & -\frac{3}{a} & -\frac{2}{a} & -\frac{1}{a} & 0 & -\frac{3}{a} & -\frac{1}{a}\\
1 & 0 & 1 & -2\alpha & 0 & 1-2\beta & 0 & -2\alpha & 0 & 1-6\beta & 0 & 0\\
0 & 0 & \frac{1}{b} & 0 & 0 & \frac{2}{b} & 0 & 0 & 0 & \frac{3}{b} & 0 & 0\\
0 & -\frac{1}{a} & 0 & 0 & -\frac{1}{a} & 0 & 0 & 0 & -\frac{1}{a} & 0 & 0 & -\frac{1}{a}
\end{bmatrix} \tag{B3}$$

Matrix $[C]$ can be inverted in symbolic form by a CAS package. Matrix elements are rather complicated to be presented in the paper.

Appendix C

Formulae for natural frequencies of simply supported plate

1. *Equilibrium of forces*
Natural vibrations are harmonic and one can write for bending deflection

$$w_b(x, y, t)=W_b(x, y)\sin\omega t, \tag{C1}$$

where ω is natural frequency. By substituting (C1) into homogeneous differential equation of motion (8), yields

$$D\Delta\Delta w_b+\omega^2 J\left(1+\frac{D\bar{m}}{SJ}\right)\Delta W_b+\omega^2\bar{m}\left(\omega^2\frac{J}{S}-1\right)W_b=0. \tag{C2}$$

Solution of Eq. (2) can be assumed in the form

$$W_b=\sin\frac{m\pi x}{a}\sin\frac{n\pi y}{b}. \tag{C3}$$

Shear deflection, according to (9), is

$$W_s=\left(-\omega^2\frac{J}{S}+\frac{D}{S}c_{mn}\right)W_b, \tag{C4}$$

and total deflection

$$W=\left(1-\omega^2\frac{J}{S}+\frac{D}{S}c_{mn}\right)W_b, \tag{C5}$$

where

$$c_{mn}=\left(\frac{m\pi}{a}\right)^2+\left(\frac{n\pi}{b}\right)^2. \tag{C6}$$

The above solution satisfy all boundary conditions for simply supported plate.

By substituting (C3) into (C2) one obtains biquadratic equation for determination of natural frequency [23]. Its solution reads

$$\omega_{mn}=\sqrt{\frac{a_{mn}}{2}-\sqrt{\left(\frac{a_{mn}}{2}\right)^2-b_{mn}}}, \tag{C7}$$

where

$$a_{mn}=\left[1+\left(1+\frac{D\bar{m}}{SJ}\right)\frac{J}{\bar{m}}c_{mn}\right]\frac{S}{J},$$
$$b_{mn}=\frac{DS}{\bar{m}J}c_{mn}^2. \tag{C8}$$

2. *Energy balance*

Natural frequencies of simply supported plate can be also determined by the energy approach. Bending strain energy, according to [1], reads

$$E_b = \frac{1}{2} D \int_0^a \int_0^b \left\{ \left(\frac{\partial^2 W_b}{\partial x^2} + \frac{\partial^2 W_b}{\partial y^2} \right)^2 - 2(1-\nu) \left[\frac{\partial^2 W_b}{\partial x^2} \frac{\partial^2 W_b}{\partial y^2} - \left(\frac{\partial^2 W_b}{\partial x \partial y} \right)^2 \right] \right\} \mathrm{d}x\mathrm{d}y. \tag{C9}$$

Substituting (C3) into (C9) one obtains after integration

$$E_b = \frac{D}{8ab} d_{mn}^2, \tag{C10}$$

where

$$d_{mn} = (m\pi)^2 \frac{b}{a} + (n\pi)^2 \frac{a}{b}. \tag{C11}$$

The shear strain energy is

$$E_s = \frac{1}{2} \int_0^a \int_0^b \left(Q_x \frac{\partial W_s}{\partial x} + Q_y \frac{\partial W_s}{\partial y} \right) \mathrm{d}x\mathrm{d}y. \tag{C12}$$

By taking into account formulae (6) and (C4), one obtains after integration

$$E_s = \frac{S}{8} \left(\frac{D}{Sa^2} \right) \left(\frac{D}{Sb^2} \right) e_{mn}, \tag{C13}$$

where

$$e_{mn} = 3(m\pi)^2 (n\pi)^2 d_{mn} + (m\pi)^6 \left(\frac{b}{a} \right)^3 + (n\pi)^6 \left(\frac{a}{b} \right)^3. \tag{C14}$$

Kinetic energy due to mass translation is,

$$E_t = \frac{1}{2} \int_0^a \int_0^b W^2 \mathrm{d}x\mathrm{d}y. \tag{C15}$$

Substituting (6) into (C4), yields after integration

$$E_t = \frac{\bar{m} ab}{8} f_{mn}^2, \tag{C16}$$

where

$$f_{mn} = 1 + \frac{D}{Sab} d_{mn}. \tag{C17}$$

Kinetic energy due to mass rotation is

$$E_r = \frac{1}{2} J \int_0^a \int_0^b \left[\left(\frac{\partial W_b}{\partial x} \right)^2 + \left(\frac{\partial W_b}{\partial y} \right)^2 \right] \mathrm{d}x\mathrm{d}y. \tag{C18}$$

Substituting (C3) into (C18) and after integration one can write

$$E_r = \frac{Jab}{8} d_{mn}. \tag{C19}$$

Natural frequency is defined as

$$\omega_{mn} = \sqrt{\frac{E_b + E_s}{E_t + E_r}}. \tag{C20}$$

Substituting corresponding expressions for strain and kinetic energy, Eqs. (C10), (C13), (C16) and (C19) into (C20) one obtains

$$\omega_{mn} = \frac{1}{ab} \sqrt{\frac{D}{\bar{m}}} \sqrt{\frac{d_{mn}^2 + \frac{D}{Sab} e_{mn}}{f_{mn}^2 + \frac{J}{\bar{m}ab} d_{mn}}}. \tag{C21}$$

Two factors in (C21) can be presented in expanded form

$$\frac{D}{Sab} = \frac{1}{6(1-\nu)k_s} \left(\frac{h}{a} \right) \left(\frac{h}{b} \right), \qquad \frac{J}{\bar{m}ab} = \frac{1}{12} \left(\frac{h}{a} \right) \left(\frac{h}{b} \right). \tag{C22}$$

Their values grow rapidly with plate thickness.

Formula (C22) for the first natural frequency ($m=n=1$) of square plate ($a=b$) takes quite simple and transparent form

$$\omega_{11} = \omega_{11}^0 \sqrt{\frac{1 + 2\pi^2 \frac{D}{Sa^2}}{\left(1 + 2\pi^2 \frac{D}{Sa^2} \right)^2 + 2\pi^2 \frac{J}{\bar{m}a^2}}}, \tag{C23}$$

where

$$\omega_{11}^0 = \frac{2\pi^2}{a^2} \sqrt{\frac{D}{\bar{m}}}, \tag{C24}$$

is the first natural frequency of thin plate.

References

[1] Szilard R. *Theories and Applications of Plate Analysis*, John Wiley & Sons: New Jersey, 2004.

[2] Mindlin RD. *J. Appl. Mech*. 1951, 18, 31–38.
[3] Mindlin RD, Schacknow A, Deresiewicz H. *J. Appl. Mech*. 1956, 23, 430–436.
[4] Liew KM, Xiang Y, Kitiporuchais S. *J. Sound Vib*. 1995, 180, 163–176.
[5] Wang CM. *ASME J. Vib. Acoust*. 1994, 116, 536–540.
[6] Shimpi RP, Patel HG. *J. Sound Vib*. 2006, 296, 979–999.
[7] Endo M, Kimura N. *J. Sound Vib*. 2007, 30, 355–373.
[8] Xing Y, Liu B. *Acta Mech. Solida Sin*. 2009, 22, 125–136.
[9] Liew KM, Xiang Y, Kitipornchai S. *Comput. Struct*. 1993, 49, 1–29.
[10] Cheung YK, Zhou D. *Comput. Struct*. 2000, 78, 757–768.
[11] Kim K, Kim BH, Choi TM, Cho DS. *Int. J. Nav. Arch. Ocean Eng*. 2012, 4, 267–280.
[12] Cho DS, Vladimir N, Choi TM. *Int. J. Nav. Arch. Ocean Eng*. 2013, 5, 478–491.
[13] Falsone G, Settineri D. *Mech. Res. Commun*. 2012, 40, 1–10.
[14] Zienkiewicz OC, Taylor RL, To JM. *Int. J. Num. Method. Eng*. 1971, 3, 275–290.
[15] Hughes TJR, Taylor RL, Kanoknukulchai W. *Int. J. Numer. Methods Eng*. 1977, 11, 1529–1543.
[16] Lee SW, Wong X. *Int. J. Num. Methods Eng*. 1982, 18, 1297–1311.
[17] Auricchio F, Taylor RL. *Finite Elem. Anal. Des*. 1995, 19, 57–68.
[18] Lovadina C. *Comput. Methods Appl. Mech. Eng*. 1998, 163, 71–85.
[19] Hughes TJR, Tezduyar T. *J. Appl. Mech*. 1981, 48, 587–596.
[20] Bathe KJ. *Finite Element Procedures*, Prentice-Hall/MIT: Englewood Cliffs, 1996.
[21] Zienkiewicz OC, Taylor RL. *The Finite Element Method*, 5th ed., Butterworth-Heinemann: Oxford, 2000.
[22] Bletzinger K, Bischoff M, Ramm E. *Comput. Struct*. 2000, 75, 321–334.
[23] Senjanović I, Vladimir N, Tomić M. *J. Sound Vib*. 2013, 332, 1868–1880.
[24] Senjanović I, Vladimir N, Hadžić N. *Mech. Res. Commun*. 2014, 55, 95–104.
[25] Senjanović I, Vladimir N, Cho DS. *Int. J. Nav. Arch. Ocean Eng*. 2015, 7, 324–345.
[26] Senjanović I, Vladimir N, Hadžić N, Tomić M. *Eng. Struct*. 2016, 110, 169–183.
[27] LS-DYNA theory manual. Livermore Software Technology Corporation, 2006.
[28] MD NASTRAN, Dynamic analysis user's guide. California, USA: Newport Beach. MSC Software, 2010.